

Published in final edited form as:

Biochim Biophys Acta. 2014 December ; 1843(12): 3018–3028. doi:10.1016/j.bbamcr.2014.09.006.

Nuclear respiratory factor 2 regulates the transcription of AMPA receptor subunit GluA2 (*Gria2*)

Anusha Priya, Kaid Johar, Bindu Nair, and Margaret T. T. Wong-Riley*

Department of Cell Biology, Neurobiology and Anatomy, Medical College of Wisconsin, 8701 Watertown Plank Road, Milwaukee, WI 53226, USA

Abstract

Neuronal activity is highly dependent on energy metabolism. Nuclear respiratory factor 2 (NRF-2) tightly couples neuronal activity and energy metabolism by transcriptionally co-regulating all 13 subunits of an important energy-generating enzyme, cytochrome c oxidase (COX), as well as critical subunits of excitatory NMDA receptors. AMPA receptors are another major class of excitatory glutamatergic receptors that mediate most of the fast excitatory synaptic transmission in the brain. They are heterotetrameric proteins composed of various combinations of GluA1-4 subunits, with GluA2 being the most common one. We have previously shown that GluA2 (*Gria2*) is transcriptionally regulated by nuclear respiratory factor 1 (NRF-1) and specificity protein 4 (Sp4), which also regulate all subunits of COX. However, it was not known if NRF-2 also couples neuronal activity and energy metabolism by regulating subunits of the AMPA receptors. By means of multiple approaches, including electrophoretic mobility shift and supershift assays, chromatin immunoprecipitation, promoter mutations, real-time quantitative PCR, and western blot analysis, NRF-2 was found to functionally regulate the expression of *Gria2*, but not of *Gria1*, *Gria3*, or *Gria4* genes in neurons. By regulating the GluA2 subunit of the AMPA receptor, NRF-2 couples energy metabolism and neuronal activity at the transcriptional level through a concurrent and parallel mechanism with NRF-1 and Sp4.

Keywords

AMPA receptor; GABP; gene regulation; GluA2; Nuclear respiratory factor 2; transcription factor

1. Introduction

The alpha-amino-3-hydroxy-5-methyl-4-isoxazolepropionic acid (AMPA) receptors are a major class of excitatory glutamatergic receptors that mediate the majority of fast excitatory

© 2014 Elsevier B.V. All rights reserved.

*Corresponding author: Margaret T. T. Wong-Riley, Ph.D., Department of Cell Biology, Neurobiology and Anatomy, Medical College of Wisconsin, 8701 Watertown Plank Road, Milwaukee, WI 53226, Telephone: 414-955-8467, Fax: 414-955-6517, mwr@mcw.edu.

Publisher's Disclaimer: This is a PDF file of an unedited manuscript that has been accepted for publication. As a service to our customers we are providing this early version of the manuscript. The manuscript will undergo copyediting, typesetting, and review of the resulting proof before it is published in its final citable form. Please note that during the production process errors may be discovered which could affect the content, and all legal disclaimers that apply to the journal pertain.

Conflict of Interest: The authors declare no competing financial interest.

synaptic transmission in the mammalian central nervous system (for review see [1]). AMPA receptors are widely expressed and are important for normal neuronal activity, including excitatory neurotransmission, synaptic plasticity, synaptic scaling, homeostatic synaptic plasticity, and learning and memory (for reviews see [2–4]). AMPA receptors are heterotetrameric proteins composed of various combinations of the GluA1, GluA2, GluA3, and GluA4 subunits (for review see [5]). The predominant AMPA receptor subtypes in the cerebral neocortex, hippocampus, and in pyramidal cells of the brain are heterotetramers containing the GluA1 and GluA2 subunits [6, 7]. The expression of the GluA3 and GluA4 subunits is much lower than that of GluA1 or GluA2, with GluA4 present mainly during development [6, 8, 9].

Glutamatergic neurotransmission is a highly energy-demanding process, with most of this energy utilized to pump out excess cations that enter the cell after glutamatergic receptor activation [10, 11]. Thus, there is an intimate link between neuronal activity and energy metabolism at the cellular level. Recently, we found that the coupling between neuronal activity and energy metabolism extends to the molecular level. The same transcription factors, nuclear respiratory factor 1 (NRF-1) and specificity protein 4 (Sp4), co-regulate energy metabolism and neuronal activity by regulating the expression of all 13 subunits of the energy-generating enzyme, cytochrome c oxidase (COX), as well as the expression of critical subunits of the excitatory AMPA and *N*-methyl-D-aspartate (NMDA) glutamatergic receptors [12–17].

Besides NRF-1, nuclear respiratory factor 2 (NRF-2) is also a transcription factor that co-regulates the expression of all 13 subunits of *COX* and critical subunits of the NMDA receptor [18–20]. It is not known, however, if NRF-2 also regulates the expression of AMPA receptor subunits. If so, three mechanisms are possible by which NRF-2 regulates the AMPA receptor subunits with respect to NRF-1 and Sp4: complementary, concurrent and parallel, or a combination of complementary and concurrent/parallel mechanisms. In the complementary mechanism, NRF-2 regulates AMPA receptor subunits complementary to those regulated by NRF-1 and Sp4. In the concurrent and parallel mechanism, NRF-2, NRF-1, and Sp4 jointly regulate the same AMPA receptor subunit genes in a parallel fashion (all are stimulatory). In a combination of the complementary and concurrent/parallel mechanisms, a subset of subunit genes is controlled by all three transcription factors, whereas another subset is controlled by NRF-2 separately from NRF-1 and Sp4.

The goal of this study was to test our hypothesis that NRF-2 regulates the same subunit genes of the AMPA receptors as NRF-1 and Sp4, and that these two transcription factors function via a concurrent and parallel mechanism.

2. Material and methods

All experiments were carried out in accordance with the US National Institutes of Health Guide for the care and use of laboratory animals and the Medical College of Wisconsin regulations. All efforts were made to minimize the number of animals and their suffering.

2.1. Cell Culture

Murine neuroblastoma (N2a) cells (ATCC® CCL-131™, Manassas, VA, USA) were grown in Dulbecco's modified Eagle's medium supplemented with 10% fetal bovine serum, 50 units/mL penicillin, and 100 µg/mL streptomycin (Invitrogen, Carlsbad, CA, USA) at 37°C in a humidified atmosphere with 5% CO₂.

Cultures of rat primary visual cortical neurons were performed according to our published protocol [19]. Briefly, 1 to 2-day old rat pups were euthanized by decapitation. Visual cortical tissue was removed, trypsinized, and triturated. Individual neurons were plated in poly-L-lysine-coated, 35 mm dishes at a density of 2×10^5 cells/dish and maintained in Neurobasal-A media supplemented with B27. Ara-C (cytosine arabinoside; Sigma, St Louis, MO, USA) was added the day after plating to suppress the proliferation of glial cells.

2.2. In silico analysis of promoters of murine AMPA receptor subunit genes

DNA sequences surrounding the transcription start point (TSP) of α -amino-3-hydroxy-5-methyl-4-isoxazolepropionic acid (AMPA) receptor subunit genes (*Gria1-4*) were derived from the NCBI mouse genome database (*Gria1* GenBank ID: NC_000077.6, *Gria2* GenBank ID: NC_000069.6, *Gria3* GenBank ID: NC_000086.7, and *Gria4* GenBank ID: NC_000075.6). Putative promoter sequences encompassing 1 kb upstream and 1 kb downstream of the TSP of each gene were analyzed. Computer-assisted search for NRF-2's binding motif 'GGAA', or its complement 'TTCC', separated by up to 24 base pairs (bp) from another such NRF-2 binding motif, was conducted on each promoter, using DNASTar Lasergene 8 Suite - Sequence Builder and Genequest software.

Alignment of human, mouse, and rat promoter sequences were performed with NCBI's Ensembl interface. Mouse AMPA receptor promoter sequences were compared with those of rat and human genomic sequences for conservation of the NRF-2 binding motif.

2.3. Electrophoretic mobility shift and supershift assays

Electrophoretic mobility shift assays (EMSA) for possible NRF-2 interactions with putative binding elements on all AMPA receptor subunit promoters were carried out with a few modifications from methods previously described [19]. Briefly, based on *in silico* analysis, oligonucleotide probes with a putative NRF-2 binding motif in a tandem repeat on each AMPA receptor subunit promoter were synthesized (Table 1A), annealed, and labeled by a Klenow fragment (Invitrogen, Grand Island, NY, USA) fill-in reaction with [α -³²P] dATP (50 µCi/200 ng; Perkin-Elmer, Shelton, CT, USA). N2a nuclear extract was isolated using methods described previously [21]. Each labeled EMSA probe was incubated with 2 µg of calf thymus DNA and 15 µg of N2a nuclear extract. The probe reaction was processed for EMSA. Supershift assays were performed with 0.4 µg of NRF-2 specific antibody (polyclonal rabbit antibody, H-180, sc-22810, Santa Cruz Biotechnology, Santa Cruz, CA, USA) added to the probe/nuclear extract mixture and incubated for 20 min at 24°C. For competition, 100-fold excess of unlabeled oligonucleotides were incubated with nuclear extract before the addition of labeled oligonucleotides. Shift reactions were loaded onto 4.5% polyacrylamide gel (58:1, Acrylamide:Bisacrylamide) and run at 200 V for 4.2 h in 0.25X Tris-borate-EDTA buffer. Results were visualized by autoradiography and exposed

on film. Rat cytochrome c oxidase subunit 6b (*COX6b*) with known NRF-2 binding site was designed as previously described [19] and used as a positive control. NRF-2 mutants with mutated sequences, as shown in Table 1B, were used as negative controls.

2.4. Chromatin immunoprecipitation (ChIP) assays in N2a cells

ChIP assays were performed similar to those described previously [15]. Briefly, 1×10^6 N2a cells were used for each immunoprecipitation reaction. Cells were fixed with 1% formaldehyde for 10 min at 24°C. Following formaldehyde fixation, cells were resuspended in swelling buffer (5 mM PIPES, pH 8.0, 85 mM KCl, and 1% Nonidet P-40 (Sigma), with protease inhibitors added right before use) and homogenized. Nuclei were then isolated and subjected to sonication in SDS lysis buffer (1% SDS, 10 mM EDTA, 50 mM Tris-HCl, pH 8.1 (Sigma)). The sonicated lysate was immunoprecipitated with either 1 µg of NRF-2 polyclonal rabbit antibody (H-180, Santa Cruz Biotechnology) or 2 µg of anti-nerve growth factor receptor (NGFR) p75 polyclonal goat antibody (C20, sc-6188, Santa Cruz Biotechnology). Semi-quantitative PCR was performed using 1/20th of precipitated chromatin. Primers encompassing putative NRF-2 tandem repeats near TSPs of AMPA receptor subunit genes (identified in *in silico* analysis) were designed (Table 2). *COX6b* promoter with NRF-2 binding site was used as a positive control [19], and exon 8 of *NRF-1*, a region of DNA that does not contain a NRF-2 binding site, was used as a negative control (Table 2). PCR reactions were carried out with DreamTaq polymerase (Thermo-Fisher Scientific, Waltham, MA, USA) and products were visualized on 2% agarose gels stained with ethidium bromide.

2.5. Chromatin immunoprecipitation (ChIP) assays from murine visual cortical tissue

ChIP assays were performed on primary neurons similar to that described for N2a cells above and as described previously [20]. Briefly, 0.1 g of murine visual cortical tissue was used for each immunoprecipitation reaction. Fresh murine visual cortex was quickly dissected and cut into small pieces. The finely chopped visual cortical tissue was fixed with 2% formaldehyde for 20 min at 24°C. Following formaldehyde fixation, cells were resuspended in swelling buffer and homogenized as described above. Nuclei isolation and immunoprecipitation, as well as the analysis of immunoprecipitated samples, including primers for positive and negative controls were identical to the ChIP protocol described for N2a cells above.

2.6. Construction and transfection of luciferase reporter vectors for promoter mutagenesis study

The *Gria2* promoter luciferase reporter construct was made by PCR cloning the *Gria2* promoter using genomic DNA prepared from mouse N2a cells as a template. Digestion with restriction enzymes MluI and BglII was followed by ligation of the product directionally into pGL3 basic luciferase vector (E1751, Promega, Madison, WI, USA). Sequences of primers used for PCR cloning are provided in Table 3A. *COX6b* clone was used from our previous study as a positive control [19]. Site-directed mutation of the putative NRF-2 tandem repeat binding site on *Gria2* was generated using QuikChange site-directed

mutagenesis kit (Stratagene, La Jolla, CA, USA). Primers for mutagenesis are listed in Table 3B. All constructs were verified by sequencing.

Each promoter construct was transfected into N2a cells in a 24-well plate using Lipofectamine 2000 (Invitrogen) and cell lysates harvested after 48 h. Each well received 0.6 μg of reporter construct and 0.06 μg of pRL-TK renilla luciferase vector (E2241, Promega), a vector with thymidine kinase (TK) promoter that constitutively expressed renilla luciferase. Transfected neurons were stimulated with KCl at a final concentration of 20 mM in the culture media for 5 h as previously described [22]. After 5 h of treatment, cell lysates were harvested and measured for luciferase activity as described previously [22]. Data from six independent transfections were averaged for each promoter construct.

2.7. Plasmid construction of NRF-2 shRNA, transfection, and KCl treatment

NRF-2 silencing was carried out using two small hairpin RNA (shRNA) sequences against murine (with identical sequences for rat) *NRF-2a* as described previously [18]. Briefly, the pBS/U6 empty parent vector was used as the negative control. The pLKO.1-puro-CMV-TurboGFP Positive Control Vector (SHC003, Sigma) containing turboGFP and puromycin resistance was used to visualize transfection efficiency and select for positively transfected cells.

For transfection of N2a cells, they were plated at 60% confluency in 6-well dishes. Cells were co-transfected the day after plating with either the *NRF-2* shRNA construct (2 μg) and turboGFP (0.5 μg) vectors or the pBS/U6 empty vector (2 μg) and the turboGFP (0.5 μg) vector using 5 μl of JetPrime transfection reagent (PolyPlus Transfection, Illkirch, France) per well. Puromycin at a final concentration of 5 $\mu\text{g}/\text{mL}$ was added to the culture medium 1.5 days after transfection to select for purely transfected cells. Green fluorescence was observed to monitor transfection efficiency. Transfection efficiency for N2a cells was around 75%; however, puromycin selection effectively yielded 100% transfected cells. N2a cells transfected with shRNA against NRF-2 were further stimulated with KCl at a final concentration of 20 mM in the culture media for 5 h as previously described [22]. After 5 h of treatment, cells were harvested for RNA isolation.

Transfection of cultured rat primary neurons was carried out 5 days post-plating with *NRF-2* shRNA constructs (2 μg) or the pLKO.1 non-mammalian control (2 μg) by means of Neurofect transfection reagent in 6-well plates according to the manufacturer's instructions (Genlantis, San Diego, CA). TurboGFP (0.5 μg) vector was added to each well for transfection visualization and selection efficiency. Transfection efficiency was around 40 – 50% before selection. Puromycin selection, however, effectively yielded 100% transfected cells. KCl stimulation was performed on rat visual cortical neurons as described for N2a cells above.

2.8. NRF-2 over-expression and TTX treatment

Vectors expressing human NRF-2 α and NRF-2 β subunits were used as described previously [18]. The empty pcDNA3.1 vector was used as a control. Transfection procedure for N2a cells and primary neuronal culture was similar to that described above. Either the NRF-2

over-expression construct (1.5 - 2 μ g) vector, or the pcDNA3.1 empty vector (1 - 1.5 μ g), and turboGFP (0.5 μ g) vectors were used, plus 5 μ l of JetPrime transfection reagent per well. Green fluorescence was used to monitor transfection efficiency. Transfected neurons were impulse blocked for 3 days with TTX at a final concentration of 0.4 μ M, starting the day after plating as previously described [22]. Four days after transfection, cells were harvested for RNA isolation.

2.9. RNA isolation and cDNA synthesis

Total RNA was isolated using TRIzol (Invitrogen) according to the manufacturer's instructions. 1 μ g of total RNA was treated with DNase I and the reaction stopped with heating at 65°C in the presence of EDTA. cDNA was synthesized using iScript cDNA synthesis kit (170-8891, BioRad, Hercules, CA, USA) according to the manufacturer's instructions.

2.10. Real-time quantitative PCR

Real-time quantitative PCR was carried out in a Cepheid Smart Cycler Detection system (Cepheid, Sunnyvale, CA, USA) and/or the iCycler System (BioRad) using the IQ Sybr Green SuperMix (170-8880, BioRad) following the manufacturer's protocols and as described previously [22]. The primer sequences used are shown in Table 5. Primers were optimized to yield 95% - 105% reaction efficiency with PCR products run on agarose gel to verify correct amplification length. Melt curve analyses verified the formation of single desired PCR product in each PCR reaction. The 2^{-CT} method was used to quantify the relative amount of transcripts [23].

2.11. Western blot Analysis

Control, NRF-2 shRNA and over-expression samples were harvested in RIPA buffer (150 mM sodium chloride, 1.0% NP-40, 0.5% sodium deoxycholate, 0.1% sodium dodecyl sulphate, 50 mM Tris, pH 8.0) with a protease inhibitor cocktail (Protease Inhibitor Cocktail III, Research Products International Corp. (RPI), Mount Prospect, IL, USA) added just before use. Samples were loaded onto 10% SDS-PAGE gel and protein was electrophoretically transferred onto polyvinylidene difluoride membranes (Bio-Rad). Subsequent to blocking, blots were incubated in primary antibodies against NRF-2 α (H-180, 1:1000, SantaCruz Biotechnology), NRF-2 β (gift of Dr. Richard Scarpulla), GluA1 (1:500; Ab1504, Millipore Chemicon, Billerica, MA, USA), GluA2 (1:200; 75-002 clone L21/32, UC Davis/NIH NeuroMab Facility, Davis, CA, USA), GluA3 (1:50; sc-7613, Santa Cruz), and GluA4 (1:50; sc-7614, Santa Cruz). β -actin (1:3000; Sigma) served as loading control. Secondary antibodies used were goat-anti-rabbit and goat-anti-mouse antibodies (Vector Laboratories, Burlingame, CA, USA). Blots were then reacted with ECL reagent (Pierce, Rockford, IL, USA) and exposed to autoradiographic film (RPI). Quantitative analyses of relative changes were done with an Alpha Imager (Alpha Innotech, San Leandro, CA, USA).

2.12. Statistical analysis

Significance among group means was determined by analysis of variance (ANOVA). Significance between two groups was analyzed by Student's *t*-test. *P*-values of 0.05 or less were considered significant.

3. Results

3.1. In silico promoter analysis of AMPA receptor subunit genes

NRF-2 binds to the 'GGAA' *cis* motif, or its complement, the 'TTCC' motif, in a tandem repeat. *In silico* analysis of the proximal promoters of murine AMPA receptor subunit genes in the DNA sequence 1 kb upstream and 1 kb downstream of the transcription start site (TSP) revealed a tandem repeat of the NRF-2 binding motifs (separated by up to 24 bp) on all subunit genes (see Table 1A for binding motifs).

3.2. In vitro binding of NRF-2 to AMPA receptor subunit promoters

To determine if NRF-2 was able to bind to putative binding sites on the AMPA promoters *in vitro*, the electrophoretic mobility shift assays (EMSA) and supershift assays were performed. Murine cytochrome c oxidase subunit 6b (*COX6b*) promoter, with a known NRF-2 binding site, served as the positive control [19]. When incubated with N2a nuclear extract, *COX6b* formed specific DNA/NRF-2 shift and supershift complexes (Fig. 1, lanes 1 and 3, respectively). When an excess of unlabeled *COX6b* probe was added as a competitor, no shift band was formed (Fig. 1, lane 2).

When AMPA receptor subunit gene promoters were tested for NRF-2 binding, only *Gria1* and *Gria2* gave positive NRF-2 shift (Fig. 1, lanes 4 and 9, respectively) and supershift bands (Fig. 1, lanes 6 and 11, respectively). Significantly, NRF-2 bound more strongly to the *Gria2* probe than to the *Gria1* probe, even though the same amount of radioactive probe was used for each reaction. The addition of unlabeled probes competed out the shift band for both *Gria1* and *Gria2* (Fig. 1, lanes 5 and 10, respectively), whereas the addition of unlabeled probes with mutated NRF-2 binding site did not compete out the specific shift bands for either gene (Fig. 1, lanes 7 and 12, respectively). Labeled probes with mutant NRF-2 sites on *Gria1* and *Gria2* did not form specific shift or NRF-2 supershift bands when incubated with N2a nuclear extract and/or NRF-2 antibody (Fig. 1, lanes 14-17, respectively). In the absence of N2a nuclear extract, NRF-2 antibody did not bind to labeled *Gria1* and *Gria2* probes (Fig. 1, lanes 8 and 13 respectively). Labeled *Gria3* and *Gria4* probes incubated with N2a extract and/or NRF-2 antibody did not reveal specific shift or supershift bands (data not shown).

3.3. In vivo interaction of NRF-2 with AMPA receptor subunit genes in N2a cells

The chromatin immunoprecipitation (ChIP) assay was performed to verify NRF-2 protein interaction with AMPA receptor subunit gene promoters *in vivo*. Sonicated nuclear lysates from N2a cells were immunoprecipitated with NRF-2 antibody and the resulting DNA was subjected to PCR analysis using primers that encompassed the putative NRF-2 binding site identified by *in silico* analysis. Immunoprecipitation with nerve growth factor receptor (NGFR) antibody and "no antibody" served as negative controls. As NRF-2 regulates

COX6b, primers against the *COX6b* gene promoter was used as a positive control for the immunoprecipitation [19]. Exon 8 of *NRF-1*, a region of DNA that does not contain a NRF-2 binding site, was used as a negative control. 0.5% and 0.1% input DNA were used as positive control for the PCR reaction. Determination of NRF-2 binding to promoter regions was done by parallel PCR amplification of all controls and immunoprecipitated samples.

As seen in Fig. 2A, agarose gel analysis of PCR products revealed specific bands for input controls in all the tested regions of the proximal AMPA receptor subunit gene promoters. The NRF-2 immunoprecipitated sample revealed an enriched band for *COX6b* positive control and *Gria2*, but not for the negative control, exon 8 of *NRF-1*. An enriched band did not occur in the NGFR or “no antibody” negative controls. There was also no enrichment of DNA in the NRF-2 immunoprecipitated samples for *Gria1*, *Gria3*, and *Gria4*.

3.4. In vivo interaction of NRF-2 with AMPA receptor subunit genes in murine visual cortex

To verify the lack of NRF-2 binding to *Gria1* was not exclusive to N2a cells, ChIP assays were also performed with sonicated nuclear extract from visual cortical tissue of wild type C6BL/J6 mice. Immunoprecipitation with NRF-2 antibody, as well as the positive and negative controls for the reaction, were similar to those of ChIP assays performed with N2a cell nuclear lysate described above.

As seen in Fig. 2B, agarose gel analysis of PCR products revealed specific bands for input controls in all the tested regions of the AMPA receptor subunit gene promoters. The NRF-2 immunoprecipitated sample revealed an enriched band for *COX6b* positive control and for *Gria2*, but not for exon 8 of *NRF-1* negative control. An enriched band did not occur in the NGFR or “no antibody” negative controls in any of the tested DNA regions. There was also no enrichment of DNA in the NRF-2 immunoprecipitated samples for *Gria1*, *Gria3*, and *Gria4*.

3.5. Effect of mutated NRF-2 binding sites on the *Gria2* and *COX6b* promoters

The proximal promoter region of *Gria2* was cloned into the pGL3 basic luciferase vector and site-directed mutagenesis of its NRF-2 tandem binding site was performed. Transfection of wild type or mutated *Gria2* promoter into N2a cells revealed a significant 66% decrease in promoter activity of the *Gria2* promoter containing the mutated NRF-2 motif ($P < 0.001$, Fig. 3). The *COX6b* promoter was used as a positive control [19]. The *COX6b* promoter containing a mutated NRF-2 motif showed a significant decrease in promoter activity ($P < 0.001$, Fig. 3).

3.6. Effect of mutated NRF-2 binding sites on the response of the *Gria2* promoter to KCl stimulation

We have shown previously that the *Gria2* promoter is up-regulated by KCl-stimulated increase in neuronal activity [13]. To verify that NRF-2 binding is necessary for this up-regulation, the control *Gria2* promoter or the *Gria2* promoter with mutated putative NRF-2 site were transfected into N2a cells. As shown in Fig. 3, N2a cells transfected with the control *Gria2* promoter and subjected to KCl depolarizing stimulation exhibited a 147% increase in promoter activity ($P < 0.001$). This increase was abolished by mutating the

NRF-2 binding site (Fig. 3), confirming a requirement for NRF-2 binding in the KCl depolarization-induced up-regulation of the *Gria2* promoter.

3.7. Effect of silencing NRF-2 by RNA interference on AMPA receptor subunits in N2a cells

To determine the effect of silencing *NRF-2a* transcript on the expression of AMPA receptor subunits, two shRNA plasmid vectors targeting *NRF-2a* mRNA were used. These vectors were previously found to silence NRF-2 expression in N2a cells [18]. The pBS/U6 empty vector was used as a control. Quantitative real-time PCR and the 2^{-CT} method were used to quantify relative *NRF-2a* and AMPA receptor subunit mRNA levels, with silenced *NRF-2a* samples compared against control samples. *Gapdh* was used as the internal control. Silencing of *NRF-2a* resulted in a 58% decrease in levels of *NRF-2a* mRNA ($P < 0.001$, Fig. 4B). There was a significant 39% decrease in mRNA levels of the positive control *COX7c* [18], and a significant 28% decrease in mRNA levels of *Gria2* ($P < 0.001$ and $P < 0.01$, respectively, Fig. 4B). Protein levels of NRF2a decreased significantly by 51% ($P < 0.001$, Fig. 4A). Protein levels of GluA2 decreased significantly by 25% ($P < 0.05$, Fig. 4A). mRNA and protein levels of *Gria1* (Fig. 4B and Fig. 4A, respectively) were not significantly changed, and neither were the mRNA and protein levels of *Gria3* and *Gria4* (Fig. 4B and Supplemental Fig. 1).

3.8. Effect of over-expressing NRF-2 on AMPA receptor subunits in N2a cells

As the functional NRF-2 transcription factor requires the DNA-binding of the α subunit as well as the transactivating β subunit, vectors over-expressing both NRF-2 α and β subunits were co-transfected into N2a cells. The pcDNA3.1 empty vector was used as a control. β -actin was used as the internal control. Over-expression of *NRF-2* α and β resulted in an approximately 30-fold and 15-fold increase in *NRF-2a* and β subunit transcripts, respectively ($P < 0.001$ for both, Fig. 5B), and a 3.5-fold and 4.25-fold increase in their protein levels, respectively ($P < 0.001$ for both, Fig. 5A). Transcript levels of the positive control, *COX7c*, increased 145.5% with NRF-2 over-expression ($P < 0.01$, Fig. 5C). *Gria2* mRNA and protein levels also increased significantly with NRF-2 over-expression to 163% and 175%, respectively ($P < 0.001$ for both, Figs. 5B and C, respectively). mRNA levels of *Gria1*, *Gria3*, and *Gria4* did not change significantly with over-expression (Fig. 5C), nor did protein levels of GluA1, GluA3, and GluA4 (Fig. 5C and Supplemental Fig. 1).

3.9. Silencing NRF-2 abolished KCl-induced transcript up-regulation of *Gria2* in N2a cells

We have previously shown that GluA2 transcript and protein levels are up-regulated in response to KCl [13]. To see if the up-regulation of *Gria2* transcript level is dependent on NRF-2 function, N2a cells transfected with pBS/U6 empty control vectors or shRNA vectors against *NRF-2* were subjected to 5 h of 20 mM KCl. Depolarizing stimuli resulted in a 212% increase in *Gria2* transcript levels ($P < 0.001$, Fig. 6A) that failed to increase in the presence of NRF-2 shRNA. Transcript levels of *COX7c* positive controls increased significantly (142%, $P < 0.001$, Fig. 6A) with KCl depolarization, but was abolished with shRNA treatment. Transcript levels of *Gria1*, *Gria3*, and *Gria4* increased significantly with KCl treatment ($P < 0.001$ for all, Fig. 6A) that remained as such in the presence of *NRF-2* shRNA treatment (Fig. 6A).

3.10. Over-expression of NRF-2 rescued tetrodotoxin-induced transcript reduction of *Gria2* in N2a cells

Our lab has previously shown that reducing neuronal activity with 0.4 μM TTX treatment also decreases transcript levels of *COX* and *Gria2* [13, 18]. To determine if NRF-2 over-expression can rescue the down-regulation of *COX* and *Gria2* induced by TTX, vectors expressing *NRF-2* α and β subunits were transfected into N2a cells that were later subjected to 0.4 μM TTX treatment for 3 days. As expected, *COX7c* and *Gria2* mRNA levels decreased to 66% and 55%, respectively ($P < 0.001$ for both, Fig. 6B). Cells transfected with *NRF-2* α and β rescued the down-regulation seen with TTX treatment, with an increase of 132% and 146%, respectively, as compared to the pcDNA3.1 empty vector controls ($P < 0.001$ for both, as compared to TTX alone; Fig. 6B). Transcript levels of *Gria1*, *Gria3*, and *Gria4* also decreased with TTX treatment but were not rescued by an over-expression of NRF-2 α/β (Fig. 6B).

3.11. Effect of silencing NRF-2 by RNA interference on AMPA receptor subunits in primary neurons

To determine if the effect seen with *NRF-2* shRNA was restricted to N2a cells, primary cultured neurons were transfected with the same shRNA, and *Gapdh* served as the internal control. *NRF-2* silencing resulted in a 58% decrease in its mRNA levels ($P < 0.01$, Fig. 7A). *Gria2*'s transcript levels were also decreased significantly by 48% ($P < 0.05$; Fig. 7A). However, *Gria1*, *Gria3*, and *Gria4* transcripts were not changed significantly with *NRF-2* silencing (Fig. 7A).

3.12. Silencing NRF-2 abolished KCl-induced transcript up-regulation of *Gria2* in primary neurons

Depolarizing stimulation with 20 mM KCl for 5 h significantly increased mRNA levels of *NRF-2*, *Gria1*, *Gria2*, *Gria3*, and *Gria4* in rat visual cortical neurons ($P < 0.01 - 0.05$; Fig. 7A). However, when neurons were transfected with *NRF-2* shRNA and stimulated with KCl, *NRF-2* and *Gria2* transcripts were significantly down-regulated to 84% and 50%, respectively ($P < 0.001$ for both; Fig. 7A), whereas those of *Gria1*, *Gria3*, and *Gria4* were not affected (Fig. 7A).

3.13. Effect of over-expressing NRF-2 on AMPA receptor subunits in primary neurons

To verify that the effect of over-expressing NRF-2 was not restricted to N2a cells, cultured rat cortical neurons were transfected with *NRF-2* α and β expression vectors. *Gapdh* served as the internal control. *NRF-2* over-expression resulted in a 186% increase in its mRNA levels ($P < 0.001$, Fig. 7B). *Gria2* mRNA levels also increased significantly by 174% with *NRF-2* over-expression ($P < 0.001$; Fig. 7B). However, *Gria1*, *Gria3*, and *Gria4* mRNA levels were not changed significantly (Fig. 7B).

3.14. Over-expression of NRF-2 rescued tetrodotoxin-induced transcript reduction of *Gria2* in primary neurons

Transcript levels of *NRF-2*, *Gria1*, *Gria2*, *Gria3*, and *Gria4* in rat visual cortical neurons were all significantly down-regulated by 0.4 μM TTX-treatment for 3 days ($P < 0.001 -$

0.01; Fig. 7B). *NRF-2* over-expression rescued *NRF-2* and *Gria2* transcripts from being down-regulated by TTX ($P < 0.001$ for both, as compared to TTX alone), but had no effect on those of *Gria1*, *Gria3*, and *Gria4* (Fig. 7B).

3.15. Homology of NRF-2 Binding Sites

The functional NRF-2 binding site on the *Gria2* promoter is conserved among mice, rats, and humans (Fig. 8).

4. Discussion

Using multiple approaches, including EMSA and supershift assays, ChIP in primary visual cortical tissue, promoter mutational analysis, over-expression and silencing studies, the present study documents for the first time that nuclear respiratory factor 2 (NRF-2) functionally regulates the expression of the AMPA receptor subunit *Gria2* (GluA2), but not *Gria1* (GluA1), *Gria3* (GluA3), or *Gria4* (GluA4) genes. Moreover, silencing of NRF-2 prevented the up-regulation of *Gria2* mRNA levels induced by depolarizing stimulation, whereas over-expression of NRF-2 rescued mRNA levels suppressed by TTX-induced impulse blockade. The NRF-2 regulatory site in the *Gria2* promoter is conserved among mice, rats, and humans.

It is important to note that even though NRF-2 binds to *Gria1* *in vitro* (EMSA), it does not do so *in vivo* (ChIP). EMSA is helpful as an initial first step in testing for possible binding site of transcription factors. However, the relatively short oligonucleotides are not in the context of a natural, cellular environment. The *in vivo* ChIP assay is necessary to confirm (or refute) that the binding is physiological. The additional functional and gene perturbation studies are also necessary to validate the functional significance of NRF-2's regulation of *Gria2*, and not of the other AMPA subunit genes.

AMPA receptors are among the most prevalent excitatory glutamatergic receptors in the brain. The majority of heterotetrameric AMPA receptors in the adult cortex and hippocampus contain the GluA2 subunit in combination with either the GluA1 or the GluA3 subunit [6, 7, 24]. The expression of GluA3 is lower than that of GluA1, and GluA1/GluA2 receptors are more prevalent than GluA2/GluA3 receptors in the adult cortex and hippocampus [6, 7, 25]. The GluA4 subunit is developmentally expressed and complexes with GluA2 in the immature hippocampus [9]. The presence or absence of GluA2 determines the major physiological properties of the AMPA receptor, including its kinetics, ion permeability, and conductance. GluA2 is unique among the AMPA subunits in that it undergoes hydrolytic editing of its pre-mRNA [26]. This editing converts a glutamine to an arginine in GluA2's critical pore-forming region and renders GluA2-containing receptors less permeable to Ca^{2+} [26–28]. GluA2-containing receptors are inwardly rectifying and exhibit low single channel conductance as compared to those that do not contain GluA2 subunits [24, 29–31]. The presence or absence of the GluA1, GluA3, and GluA4 subunits do not alter the properties of the AMPA receptor to the same extent as the presence or absence of GluA2.

GluA2 knockout mice exhibit multiple behavioral abnormalities, including deficits in object exploration, grooming, eye-closure reflex, and spatial and non-spatial learning [32]. A mechanism for the maintenance of long-term potentiation (LTP), the prototypical form of synaptic plasticity thought to underlie information storage and experience-dependent plasticity, can be through an increase in GluA2-containing receptors at hippocampal synapses [33–35]. In some regions of the brain, another form of synaptic plasticity, long-term depression (LTD), is thought to require the GluA2 subunit [36, 37]. Thus, the GluA2 subunit is important for normal neuronal activities including synaptic plasticity, learning, and memory.

The GluA2 subunit responds to changes in neuronal activity. Our laboratory has shown that both transcript and protein expressions of GluA2 in cultured visual cortical neurons are up-regulated by physiological concentrations of KCl [38]. Likewise, TTX-induced impulse blockade leads to a down-regulation of GluA2 mRNA and protein levels [38]. Furthermore, concurrent with neuronal activity-mediated changes in GluA2 transcript and protein levels is a parallel change in protein and transcript levels of cytochrome c oxidase (COX), a critical enzyme for energy generation in neurons [38]. In the supragranular and infragranular layers of the macaque visual cortex, GluA2 levels are governed by visual input and neuronal activity [39]. Monocular impulse blockade induces a down-regulation of GluA2 in deprived ocular dominance columns, where the activity level of COX is also reduced [39]. Thus, GluA2 and COX are tightly regulated at the cellular level. As the bulk of energy in neurons is used for repolarizing membrane potentials after excitatory depolarization [10, 11], the level of GluA2 will affect the level of neuronal activity, hence, the energy demand of neurons.

The current study shows that a molecular mechanism for the parallel regulation of *COX* and *Gria2* is through nuclear respiratory factor 2 (NRF-2), an *Ets* family transcription factor that is the human homologue of the murine GA binding protein (GABP) (for review see [40]). The functional NRF-2 protein is a heterodimer or a heterotetramer of the α and β subunits [41]. The α subunit contains the DNA binding domain that binds to the GGAA *cis*- element [41, 42]. The β subunit contains the transactivating domain and mediates heterodimer ($\alpha\beta$) or heterotetramer ($\alpha_2\beta_2$) formation, the latter being induced by homodimerization of two β subunits [42, 43]. With increased neuronal activity, NRF-2 α and β levels are up-regulated with a nuclear translocation of the subunits [44–46]. Our previous studies have shown that NRF-2 regulates all 13 subunits of *COX* and also couples neuronal activity and energy metabolism by regulating critical subunits of the excitatory glutamatergic NMDA receptors [18–20].

Previously, we have shown that the expression of the GluA2 subunit is also regulated by nuclear respiratory factor 1 (NRF-1) and specificity protein 4 (Sp4), transcription factors that regulate all 13 subunits of *COX* [12–14, 16]. Thus, the mechanism employed by NRF-2 with respect to NRF-1 and Sp4 in regulating the GluA2, but not GluA1, GluA3, or GluA4 subunits, is the concurrent and parallel mechanism rather than the complementary one.

It has recently been shown that excessive activation of AMPA receptors by glutamate is involved in neuronal excitotoxicity [47, 48]. In diseases such as amyotrophic lateral

sclerosis and ischemia, activation of AMPA receptors can lead to excitotoxic cell death [47, 49, 50]. The entry of excessive Ca^{2+} ions often triggers excitotoxic neuronal damage, and Ca^{2+} permeable AMPA receptors play an important role in AMPA receptor-mediated excitotoxicity [47–50]. Incorporation of the GluA2 subunit, however, substantially reduces the Ca^{2+} permeability of the AMPA receptor [28]. The current work, as well as past studies by this laboratory, show that GluA2 mRNA and protein levels are coupled to neuronal activity at the transcriptional level [13, 14, 18, 19]. The concurrent and parallel mechanism of transcriptional coupling of the GluA2 subunit with energy metabolism by NRF-1, NRF-2, and Sp4 may be a mechanism by which neurons can limit the entry of Ca^{2+} ions under conditions of increased neuronal activity and protect them from potential damage caused by Ca^{2+} -induced excitotoxicity.

Although NRF-1, NRF-2, and Sp4 co-regulate GluA2 via a concurrent and parallel mechanism, it is unlikely that they function in a redundant manner. First, knockout of either NRF-1 or NRF-2 is embryonically lethal, and silencing of one does not affect the expression of the other [14, 18]. While knockout of Sp4 is not lethal, the neurological deficits seen with a lack of Sp4 were not compensated for by any other transcription factor [51, 52]. Second, a virtually identical pattern of COX activity and NRF-2 α expression exists in the macaque visual cortex, under both normal and functionally perturbed states [45, 53, 54]. Such was not the case for NRF-1 (our unpublished observations). Third, both NRF-1 and NRF-2 interact with peroxisome proliferator-activated receptor- γ coactivator 1 α (PGC-1 α) to co-operatively enhance the transcription of target genes [55]. PGC-1 α is a transcriptional co-activator regulated by neuronal activity, and it potently induces mRNA and protein expressions of NRF-1 and NRF-2 [55–57]. However, whereas PGC-1 α interacts directly with NRF-1, it does so indirectly with NRF-2 through a co-regulator, host cell factor 1 (HCF-1) [55, 58]. Direct interactions of PGC-1 α with Sp4 is not reported, but Sp1, a transcription factor in the same family as Sp4, is known to interact with HCF-1 [59]. The presence of an intermediate in the PGC-1 α and NRF-2 interaction, as well as a possible intermediate in the PGC-1 α and Sp4 interaction, suggests that NRF-1, NRF-2, and Sp4 operate slightly differently in the co-regulation of neuronal activity and energy metabolism. Elucidating the mechanisms of such regulation will help to further our understanding of the differential and non-redundant roles played by these transcription factors in neurons.

We have previously shown that genes of all nucleus-encoded subunits of COX and that of *Gria2* (as well as of NMDA receptors) are transcribed in close physical proximity, i.e., in the same transcription factory within the nucleus [60]. NRF-2, NRF-1, and Sp4's concurrent and parallel mechanism of regulation makes it likely that the transcription factors exist within the same transcription factory to regulate gene expression, at least at the basal level, in neurons. Chromosomal interactions are also affected by changes in neuronal activity [60]. The fact that NRF-2 (the present study), NRF-1 [13], and Sp4 [61] respond to such changes themselves suggests that their regulation in neurons is highly dynamic.

Supplementary Material

Refer to Web version on PubMed Central for supplementary material.

Acknowledgments

This work is supported by NIH Grant R01 EY018441 and NIH/NEI Training Grant 1-T32-EY14537. Anusha Priya is a member of the MCW-MSTP, which is partially supported by a T32 grant from NIGMS, GM080202.

Abbreviations

NRF-2	nuclear respiratory factor 2
Gria	gene name for AMPA receptor subunit

References

1. Isaac JT, Ashby MC, McBain CJ. The role of the GluR2 subunit in AMPA receptor function and synaptic plasticity. *Neuron*. 2007; 54:859–871. [PubMed: 17582328]
2. Malinow R, Malenka RC. AMPA receptor trafficking and synaptic plasticity. *Annu Rev Neurosci*. 2002; 25:103–126. [PubMed: 12052905]
3. Turrigiano GG. The self-tuning neuron: synaptic scaling of excitatory synapses. *Cell*. 2008; 135:422–435. [PubMed: 18984155]
4. Shepherd JD, Huganir RL. The cell biology of synaptic plasticity: AMPA receptor trafficking. *Annu Rev Cell Dev Biol*. 2007; 23:613–643. [PubMed: 17506699]
5. Borges K, Dingledine R. AMPA receptors: molecular and functional diversity. *Prog Brain Res*. 1998; 116:153–170. [PubMed: 9932376]
6. Wenthold RJ, Petralia RS, Blahos J II, Niedzielski AS. Evidence for multiple AMPA receptor complexes in hippocampal CA1/CA2 neurons. *J Neurosci*. 1996; 16:1982–1989. [PubMed: 8604042]
7. Craig AM, Blackstone CD, Huganir RL, Banker G. The distribution of glutamate receptors in cultured rat hippocampal neurons: postsynaptic clustering of AMPA-selective subunits. *Neuron*. 1993; 10:1055–1068. [PubMed: 7686378]
8. Petralia RS, Wenthold RJ. Light and electron immunocytochemical localization of AMPA-selective glutamate receptors in the rat brain. *J Comp Neurol*. 1992; 318:329–354. [PubMed: 1374769]
9. Zhu JJ, Esteban JA, Hayashi Y, Malinow R. Postnatal synaptic potentiation: delivery of GluR4-containing AMPA receptors by spontaneous activity. *Nat Neurosci*. 2000; 3:1098–1106. [PubMed: 11036266]
10. Wong-Riley MT. Bigenomic regulation of cytochrome C oxidase in neurons and the tight coupling between neuronal activity and energy metabolism. *Adv Exp Med Biol*. 2012; 748:283–304. [PubMed: 22729863]
11. Wong-Riley MT. Cytochrome oxidase: an endogenous metabolic marker for neuronal activity. *Trends Neurosci*. 1989; 12:94–101. [PubMed: 2469224]
12. Priya A, Johar K, Nair B, Wong-Riley MT. Specificity protein 4 (Sp4) regulates the transcription of AMPA receptor subunit GluA2 (Gria2). *Biochim Biophys Acta*. 2014; 1843:1196–1206. [PubMed: 24576410]
13. Dhar SS, Liang HL, Wong-Riley MT. Nuclear respiratory factor 1 co-regulates AMPA glutamate receptor subunit 2 and cytochrome c oxidase: tight coupling of glutamatergic transmission and energy metabolism in neurons. *J Neurochem*. 2009; 108:1595–1606. [PubMed: 19166514]
14. Dhar SS, Ongwijitwat S, Wong-Riley MT. Nuclear respiratory factor 1 regulates all ten nuclear-encoded subunits of cytochrome c oxidase in neurons. *J Biol Chem*. 2008; 283:3120–3129. [PubMed: 18077450]
15. Dhar SS, Wong-Riley MT. Coupling of energy metabolism and synaptic transmission at the transcriptional level: role of nuclear respiratory factor 1 in regulating both cytochrome c oxidase and NMDA glutamate receptor subunit genes. *J Neurosci*. 2009; 29:483–492. [PubMed: 19144849]

16. Johar K, Priya A, Dhar S, Liu Q, Wong-Riley MT. Neuron-specific specificity protein 4 bigenomically regulates the transcription of all mitochondria- and nucleus-encoded cytochrome c oxidase subunit genes in neurons. *J Neurochem*. 2013; 127:496–508. [PubMed: 24032355]
17. Priya A, Johar K, Wong-Riley MT. Specificity protein 4 functionally regulates the transcription of NMDA receptor subunits GluN1, GluN2A, and GluN2B. *Biochim Biophys Acta*. 2013; 1833:2745–2756. [PubMed: 23871830]
18. Ongwijitwat S, Liang HL, Graboyes EM, Wong-Riley MT. Nuclear respiratory factor 2 senses changing cellular energy demands and its silencing down-regulates cytochrome oxidase and other target gene mRNAs. *Gene*. 2006; 374:39–49. [PubMed: 16516409]
19. Ongwijitwat S, Wong-Riley MT. Is nuclear respiratory factor 2 a master transcriptional coordinator for all ten nuclear-encoded cytochrome c oxidase subunits in neurons? *Gene*. 2005; 360:65–77. [PubMed: 16126350]
20. Priya A, Johar K, Wong-Riley MT. Nuclear respiratory factor 2 regulates the expression of the same NMDA receptor subunit genes as NRF-1: both factors act by a concurrent and parallel mechanism to couple energy metabolism and synaptic transmission. *Biochim Biophys Acta*. 2013; 1833:48–58. [PubMed: 23085505]
21. Abmayr SM, Yao T, Parmely T, Workman JL. Preparation of nuclear and cytoplasmic extracts from mammalian cells. *Curr Protoc Mol Biol*. 2006; Chapter 12 Unit 12 11.
22. Dhar SS, Liang HL, Wong-Riley MT. Transcriptional coupling of synaptic transmission and energy metabolism: role of nuclear respiratory factor 1 in co-regulating neuronal nitric oxide synthase and cytochrome c oxidase genes in neurons. *Biochim Biophys Acta*. 2009; 1793:1604–1613. [PubMed: 19615412]
23. Livak KJ, Schmittgen TD. Analysis of relative gene expression data using real-time quantitative PCR and the 2⁻(Delta Delta C(T)) Method. *Methods*. 2001; 25:402–408. [PubMed: 11846609]
24. Geiger JR, Melcher T, Koh DS, Sakmann B, Seeburg PH, Jonas P, Monyer H. Relative abundance of subunit mRNAs determines gating and Ca²⁺ permeability of AMPA receptors in principal neurons and interneurons in rat CNS. *Neuron*. 1995; 15:193–204. [PubMed: 7619522]
25. Sans N, Vissel B, Petralia RS, Wang YX, Chang K, Royle GA, Wang C'Y, O'Gorman S, Heinemann SF, Wenthold RJ. Aberrant formation of glutamate receptor complexes in hippocampal neurons of mice lacking the GluR2 AMPA receptor subunit. *J Neurosci*. 2003; 23:9367–9373. [PubMed: 14561864]
26. Sommer B, Kohler M, Sprengel R, Seeburg PH. RNA editing in brain controls a determinant of ion flow in glutamate-gated channels. *Cell*. 1991; 67:11–19. [PubMed: 1717158]
27. Higuchi M, Single FN, Kohler M, Sommer B, Sprengel R, Seeburg PH. RNA editing of AMPA receptor subunit GluR-B: a base-paired intron-exon structure determines position and efficiency. *Cell*. 1993; 75:1361–1370. [PubMed: 8269514]
28. Dingledine R, Borges K, Bowie D, Traynelis SF. The glutamate receptor ion channels. *Pharmacol Rev*. 1999; 51:7–61. [PubMed: 10049997]
29. Laezza F, Dingledine R. Voltage-controlled plasticity at GluR2-deficient synapses onto hippocampal interneurons. *J Neurophysiol*. 2004; 92:3575–3581. [PubMed: 15331617]
30. Hestrin S. Different glutamate receptor channels mediate fast excitatory synaptic currents in inhibitory and excitatory cortical neurons. *Neuron*. 1993; 11:1083–1091. [PubMed: 7506044]
31. Kamboj SK, Swanson GT, Cull-Candy SG. Intracellular spermine confers rectification on rat calcium-permeable AMPA and kainate receptors. *J Physiol*. 1995; 486(Pt 2):297–303. [PubMed: 7473197]
32. Gerlai R, Henderson JT, Roder JC, Jia Z. Multiple behavioral anomalies in GluR2 mutant mice exhibiting enhanced LTP. *Behav Brain Res*. 1998; 95:37–45. [PubMed: 9754875]
33. Liu SQ, Cull-Candy SG. Synaptic activity at calcium-permeable AMPA receptors induces a switch in receptor subtype. *Nature*. 2000; 405:454–458. [PubMed: 10839540]
34. Liu SJ, Cull-Candy SG. Activity-dependent change in AMPA receptor properties in cerebellar stellate cells. *J Neurosci*. 2002; 22:3881–3889. [PubMed: 12019307]
35. Plant K, Pelkey KA, Bortolotto ZA, Morita D, Terashima A, McBain CJ, Collingridge GL, Isaac JT. Transient incorporation of native GluR2-lacking AMPA receptors during hippocampal long-term potentiation. *Nat Neurosci*. 2006; 9:602–604. [PubMed: 16582904]

36. Chung HJ, Steinberg JP, Haganir RL, Linden DJ. Requirement of AMPA receptor GluR2 phosphorylation for cerebellar long-term depression. *Science*. 2003; 300:1751–1755. [PubMed: 12805550]
37. Toyoda H, Wu LJ, Zhao MG, Xu H, Jia Z, Zhuo M. Long-term depression requires postsynaptic AMPA GluR2 receptor in adult mouse cingulate cortex. *J Cell Physiol*. 2007; 211:336–343. [PubMed: 17149707]
38. Bai X, Wong-Riley MT. Neuronal activity regulates protein and gene expressions of GluR2 in postnatal rat visual cortical neurons in culture. *J Neurocytol*. 2003; 32:71–78. [PubMed: 14618102]
39. Wong-Riley MT, Jacobs P. AMPA glutamate receptor subunit 2 in normal and visually deprived macaque visual cortex. *Vis Neurosci*. 2002; 19:563–573. [PubMed: 12507323]
40. Rosmarin AG, Resendes KK, Yang Z, McMillan JN, Fleming SL. GA-binding protein transcription factor: a review of GABP as an integrator of intracellular signaling and protein-protein interactions. *Blood Cells Mol Dis*. 2004; 32:143–154. [PubMed: 14757430]
41. Batchelor AH, Piper DE, de la Brousse FC, McKnight SL, Wolberger C. The structure of GABPalpha/beta: an ETS domain-ankyrin repeat heterodimer bound to DNA. *Science*. 1998; 279:1037–1041. [PubMed: 9461436]
42. LaMarco K, Thompson CC, Byers BP, Walton EM, McKnight SL. Identification of Ets- and notch-related subunits in GA binding protein. *Science*. 1991; 253:789–792. [PubMed: 1876836]
43. de la Brousse FC, Birkenmeier EH, King DS, Rowe LB, McKnight SL. Molecular and genetic characterization of GABP beta. *Genes Dev*. 1994; 8:1853–1865. [PubMed: 7958862]
44. Yang SJ, Liang HL, Ning G, Wong-Riley MT. Ultrastructural study of depolarization-induced translocation of NRF-2 transcription factor in cultured rat visual cortical neurons. *Eur J Neurosci*. 2004; 19:1153–1162. [PubMed: 15016074]
45. Wong-Riley MT, Yang SJ, Liang HL, Ning G, Jacobs P. Quantitative immuno-electron microscopic analysis of nuclear respiratory factor 2 alpha and beta subunits: Normal distribution and activity-dependent regulation in mammalian visual cortex. *Vis Neurosci*. 2005; 22:1–18. [PubMed: 15842736]
46. Zhang C, Wong-Riley MT. Depolarizing stimulation upregulates GA-binding protein in neurons: a transcription factor involved in the bigenomic expression of cytochrome oxidase subunits. *Eur J Neurosci*. 2000; 12:1013–1023. [PubMed: 10762332]
47. Gorter JA, Petrozzino JJ, Aronica EM, Rosenbaum DM, Opitz T, Bennett MV, Connor JA, Zukin RS. Global ischemia induces downregulation of Glur2 mRNA and increases AMPA receptor-mediated Ca²⁺ influx in hippocampal CA1 neurons of gerbil. *J Neurosci*. 1997; 17:6179–6188. [PubMed: 9236229]
48. Liu SJ, Zukin RS. Ca²⁺-permeable AMPA receptors in synaptic plasticity and neuronal death. *Trends Neurosci*. 2007; 30:126–134. [PubMed: 17275103]
49. Buckingham SD, Kwak S, Jones AK, Blackshaw SE, Sattelle DB. Edited GluR2, a gatekeeper for motor neurone survival? *Bioessays*. 2008; 30:1185–1192. [PubMed: 18937367]
50. Kwak S, Weiss JH. Calcium-permeable AMPA channels in neurodegenerative disease and ischemia. *Curr Opin Neurobiol*. 2006; 16:281–287. [PubMed: 16698262]
51. Gollner H, Bouwman P, Mangold M, Karis A, Braun H, Rohner I, Del Rey A, Besedovsky HO, Meinhardt A, van den Broek M, Cutforth T, Grosveld F, Philipson S, Suske G. Complex phenotype of mice homozygous for a null mutation in the Sp4 transcription factor gene. *Genes Cells*. 2001; 6:689–697. [PubMed: 11532028]
52. Supp DM, Witte DP, Branford WW, Smith EP, Potter SS. Sp4, a member of the Sp1-family of zinc finger transcription factors, is required for normal murine growth, viability, and male fertility. *Dev Biol*. 1996; 176:284–299. [PubMed: 8660867]
53. Nie F, Wong-Riley M. Nuclear respiratory factor-2 subunit protein: correlation with cytochrome oxidase and regulation by functional activity in the monkey primary visual cortex. *J Comp Neurol*. 1999; 404:310–320. [PubMed: 9952350]
54. Guo A, Nie F, Wong-Riley M. Human nuclear respiratory factor 2 alpha subunit cDNA: isolation, subcloning, sequencing, and in situ hybridization of transcripts in normal and monocularly deprived macaque visual system. *J Comp Neurol*. 2000; 417:221–232. [PubMed: 10660899]

55. Wu Z, Puigserver P, Andersson U, Zhang C, Adelmant G, Mootha V, Troy A, Cinti S, Lowell B, Scarpulla RC, Spiegelman BM. Mechanisms controlling mitochondrial biogenesis and respiration through the thermogenic coactivator PGC-1. *Cell*. 1999; 98:115–124. [PubMed: 10412986]
56. Meng H, Liang HL, Wong-Riley M. Quantitative immuno-electron microscopic analysis of depolarization-induced expression of PGC-1alpha in cultured rat visual cortical neurons. *Brain Res*. 2007; 1175:10–16. [PubMed: 17870059]
57. Liang HL, Dhar SS, Wong-Riley MT. p38 mitogen-activated protein kinase and calcium channels mediate signaling in depolarization-induced activation of peroxisome proliferator-activated receptor gamma coactivator-1alpha in neurons. *J Neurosci Res*. 2010; 88:640–649. [PubMed: 19774670]
58. Vercauteren K, Gleyzer N, Scarpulla RC. PGC-1-related coactivator complexes with HCF-1 and NRF-2beta in mediating NRF-2(GABP)-dependent respiratory gene expression. *J Biol Chem*. 2008; 283:12102–12111. [PubMed: 18343819]
59. Gunther M, Laithier M, Brison O. A set of proteins interacting with transcription factor Sp1 identified in a two-hybrid screening. *Mol Cell Biochem*. 2000; 210:131–142. [PubMed: 10976766]
60. Dhar SS, Wong-Riley MT. Chromosome conformation capture of transcriptional interactions between cytochrome c oxidase genes and genes of glutamatergic synaptic transmission in neurons. *J Neurochem*. 2010; 115:676–683. [PubMed: 21064266]
61. Johar K, Priya A, Wong-Riley MT. Regulation of Na(+)/K(+)-ATPase by neuron-specific transcription factor Sp4: implication in the tight coupling of energy production, neuronal activity and energy consumption in neurons. *Eur J Neurosci*. 2013; 39:566–578. [PubMed: 24219545]

Highlights

- NRF-2 regulates the critical GluA2 (*Gria2*) subunit gene of AMPA receptors
- NRF-2 silencing prevented *Gria2* transcript's up-regulation by KCl depolarization
- Over-expressing NRF-2 rescued TTX-mediated down-regulation of *Gria2* transcripts
- NRF-2 regulates *Gria2* via a concurrent and parallel mechanism with NRF-1 and Sp4
- NRF-2 transcriptionally co-regulates energy metabolism and neuronal activity

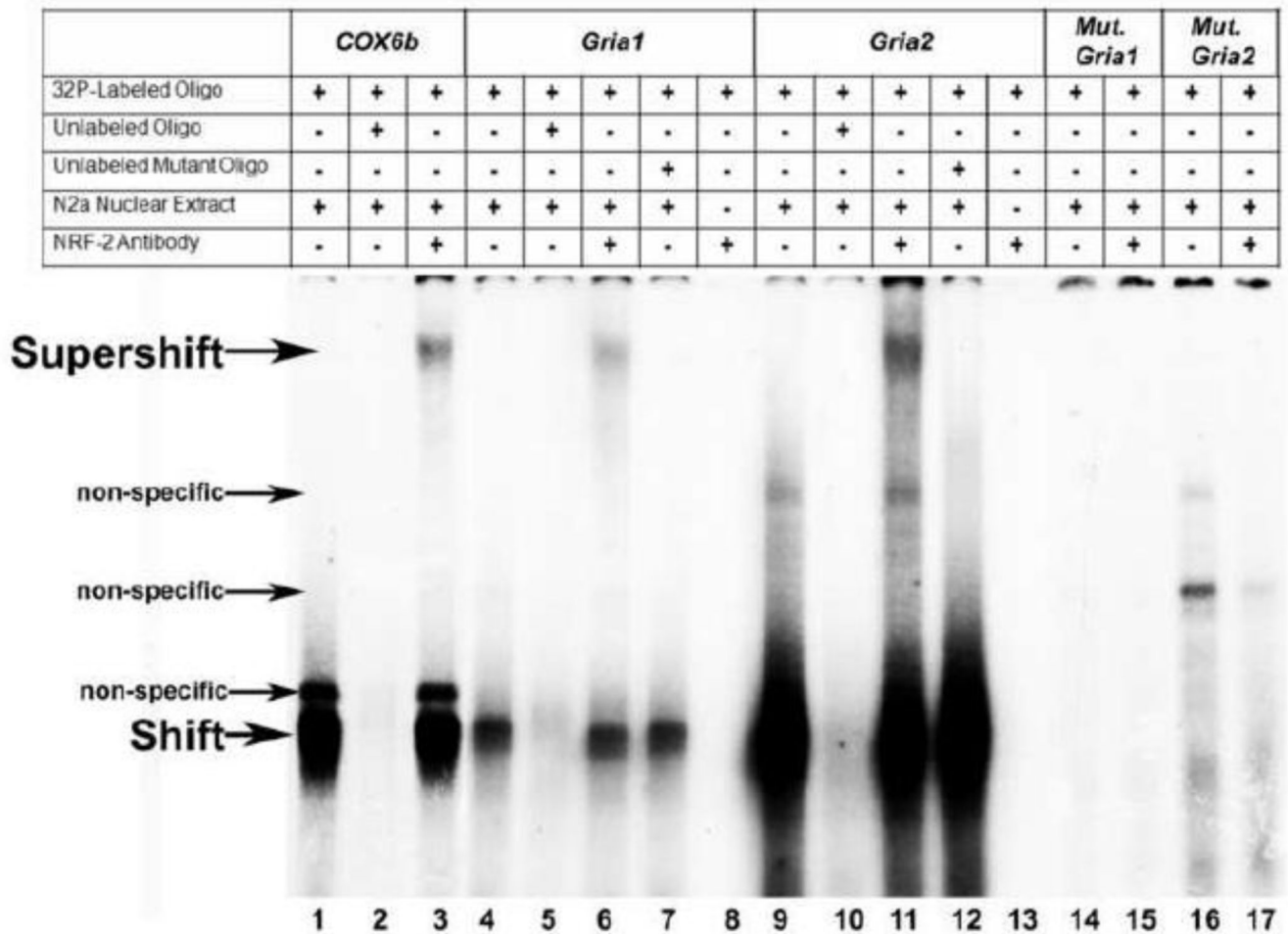


Figure 1.

In vitro binding of NRF-2 to putative binding sites on the AMPA receptor subunit gene promoters as determined with EMSA and supershift assays. ³²P-labeled oligonucleotides, excess unlabeled oligos as competitors, excess unlabeled mutant NRF-2 oligos as competitors, N2a nuclear extract, and NRF-2 α antibodies are indicated by a + or a - sign. Arrowheads indicate specific NRF-2 shift, supershift, and non-specific complexes. The positive control, *COX6b*, shows a shift and supershift band (lanes 1 and 3, respectively). The addition of excess unlabeled probe competed out the shift band (lane 2). The addition of N2a nuclear extract yielded specific shift bands for both *Gria1* and *Gria2* (lanes 4 and 9, respectively) that were competed out by an excess of unlabeled oligos (lanes 5 and 10, respectively). The addition of NRF-2 antibody yielded a supershift band for both *Gria1* and *Gria2* (lanes 6 and 11, respectively). The addition of excess unlabeled probes with mutated NRF-2 binding sites did not compete out the shift reaction (lanes 7 and 12, respectively). The addition of NRF-2 antibody to labeled *Gria1* and *Gria2* probes in the absence of N2a extract did not reveal any antibody-to-probe reaction (lanes 8 and 13, respectively). Labeled *Gria1* and *Gria2* probes with mutated NRF-2 sites did not yield a specific NRF-2 shift band (lanes 14 and 16, respectively), nor a supershift band with the addition of NRF-2 antibody (lanes 15 and 17, respectively).

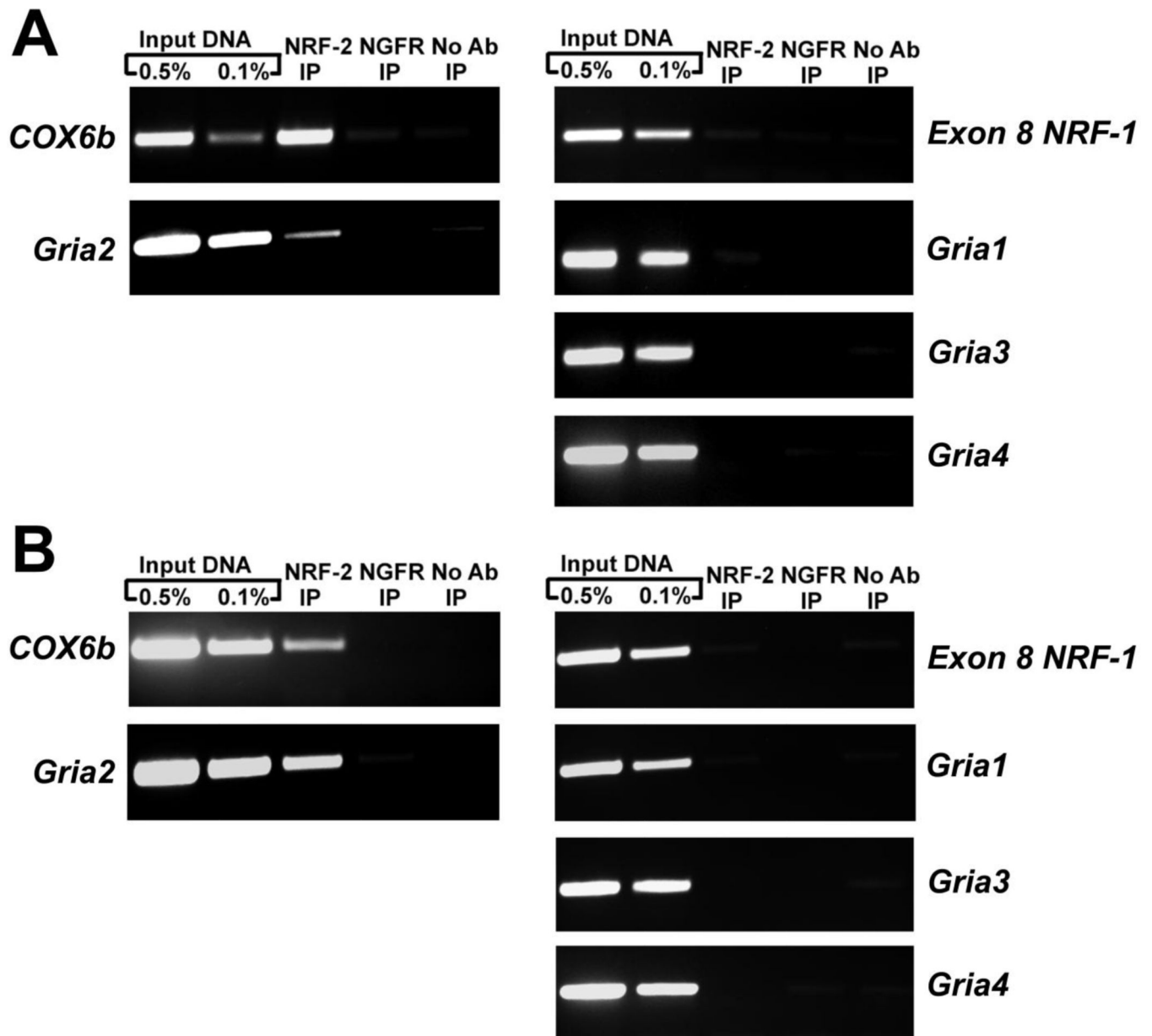


Figure 2.

In vivo interaction of NRF-2 with the AMPA receptor subunit gene promoters using the ChIP assay in N2a cells (A) and murine visual cortical tissue (B). Nuclear extract was immunoprecipitated with anti NRF-2 α antibodies (NRF-2 IP lane), anti-nerve growth factor receptor p75 antibody (negative control, NGFR IP lane), or no antibody (negative control, No Ab lane). Control reactions for PCR were performed with 0.5% (Input 0.5% IP lane) and 0.1% (Input 0.1% IP lane) of input chromatin. *COX6B* promoter was used as a positive control, and Exon 8 of NRF-1 was used as a negative control. Results indicate NRF-2 interactions with the tested region on the *Gria2* promoter, but not the *Gria1*, *Gria3*, or *Gria4* promoters, in both N2a cells and murine visual cortical tissue.

Relative Luciferase Activity

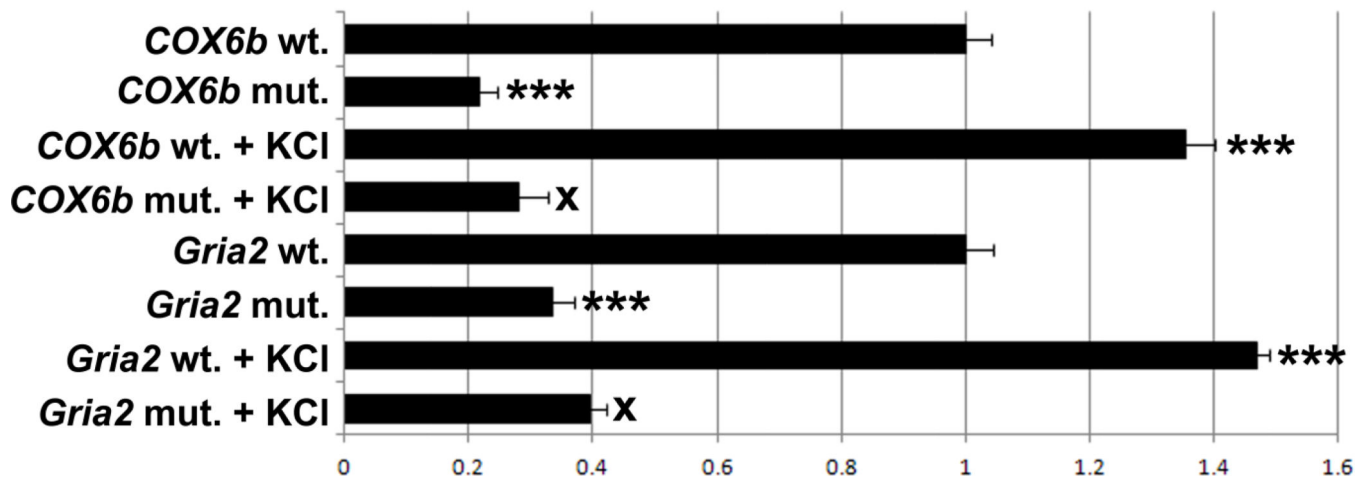


Figure 3.

Site-directed mutational analysis of promoters using luciferase reporter gene constructs.

Wild type promoters (wt) and those with mutated NRF-2 binding site (mut) for *COX6b* and *Gria2* are indicated. *COX6b* served as a positive control. Mutating the NRF-2 site resulted in a significant decrease in the luciferase activity as compared to the wild type. Similarly, mutating the NRF-2 binding sites on the *Gria2* promoter resulted in significant decreases in luciferase activity. KCl depolarization significantly increased promoter activity in all wild type, but not in the *COX6b* and *Gria2* promoters with mutated NRF-2 sites. $N = 6$ for each construct. ***= $P < 0.001$; X = NS. All mutants and wild type + KCl are compared to the wild type. All mutant + KCl are compared to mutants.

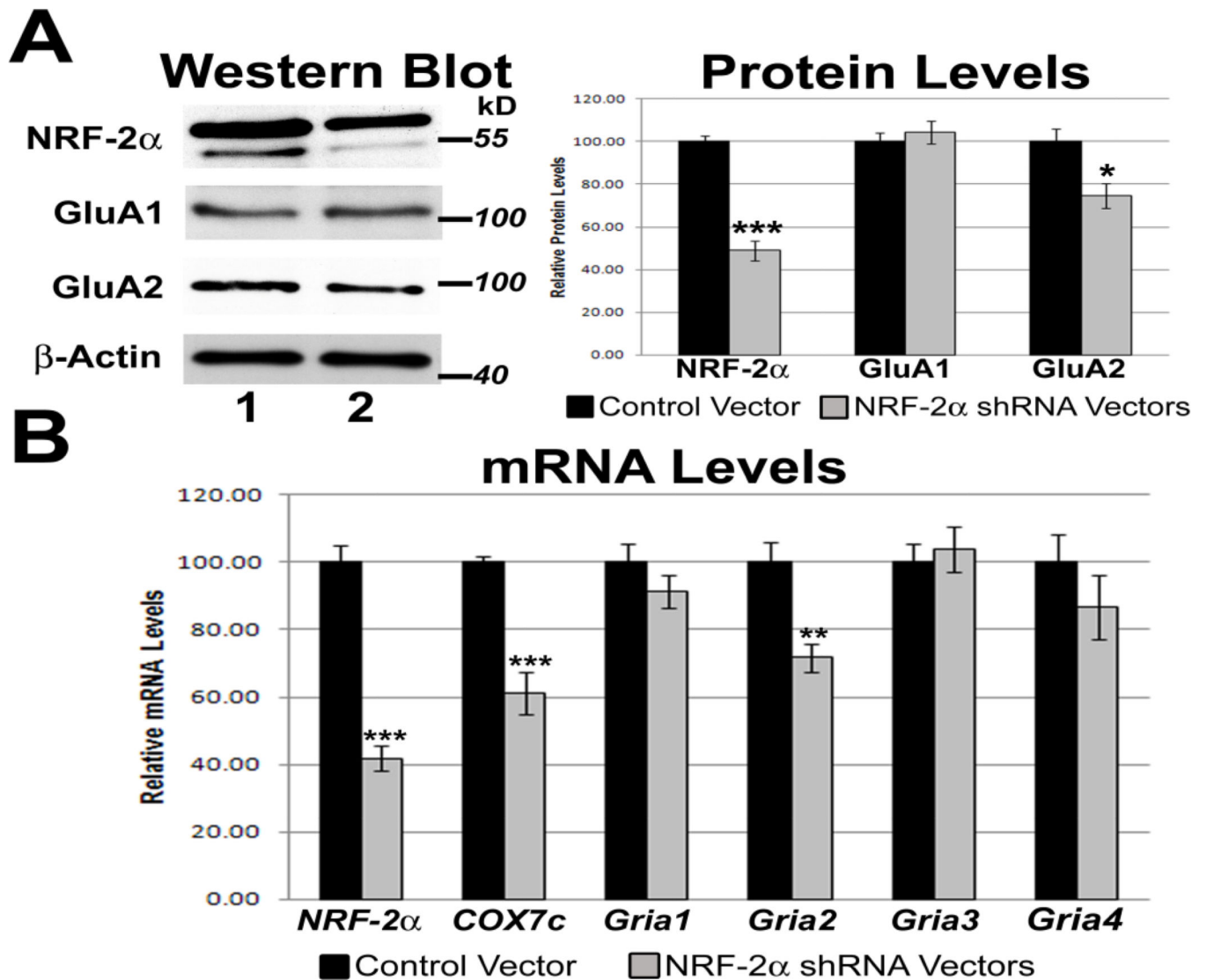


Figure 4. Effect of RNA interference-mediated silencing of NRF-2 α on the expression of COX and AMPA receptor subunit genes. (A) Western blots revealed a down-regulation of NRF-2 α and GluA2 protein levels (lane 2) as compared to controls (lane 1), but not GluA1 protein levels, in NRF-2 α shRNA-transfected cells. β -actin served as a loading control. N = 3 for each data point; ***= $P < 0.001$ and *= $P < 0.05$ when compared to pBS/U6 empty vector controls. (B) As determined by real-time PCR, NRF-2 α shRNA transfection in N2a cells down-regulated mRNA levels of NRF-2 α and *Gria2*, but not those of *Gria1*, *Gria3*, and *Gria4*. mRNA levels of the positive control, *COX7c*, were also reduced with NRF-2 α silencing. N = 6 for each data point. ***= $P < 0.001$ and **= $P < 0.01$ when compared to pBS/U6 empty vector controls.

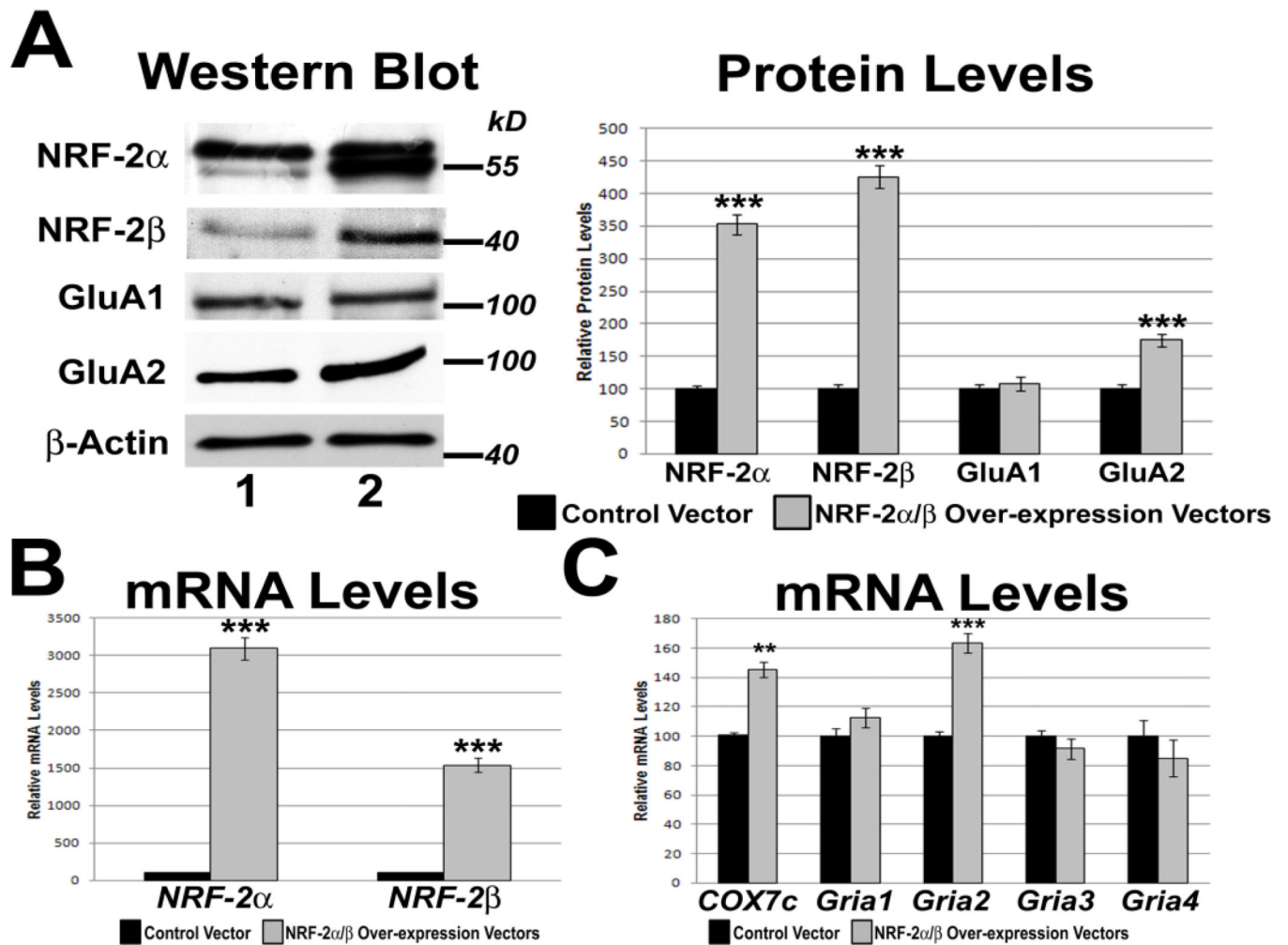


Figure 5. Effect of over-expressing NRF-2α and β on the transcript and protein levels of *COX7c* and AMPA receptor subunit genes. (A) NRF-2α/β over-expression increased protein levels of NRF-2α and NRF-2β, as well as GluA2 (lane 2) as compared to controls (lane 1). Protein levels of GluA1 did not increase significantly with NRF-2α/β over-expression. β-actin served as a loading control. N = 3 for each data point; ***= $P < 0.001$ when compared to pcDNA3.1 empty vector controls. (B) Real-time PCR revealed an up-regulation of *NRF-2α* and *β* mRNA with NRF-2α/β over-expression as compared to pcDNA3.1 empty vector controls. (C) In N2a cells, mRNA levels of *Gria2*, but not those of *Gria1*, *Gria3*, and *Gria4*, were increased with NRF-2α/β over-expression. mRNA levels of the positive control, *COX7c*, were also increased with NRF-2α/β over-expression. N = 6 for each data point. **= $P < 0.01$ and ***= $P < 0.001$ when compared to pcDNA3.1 empty vector controls.

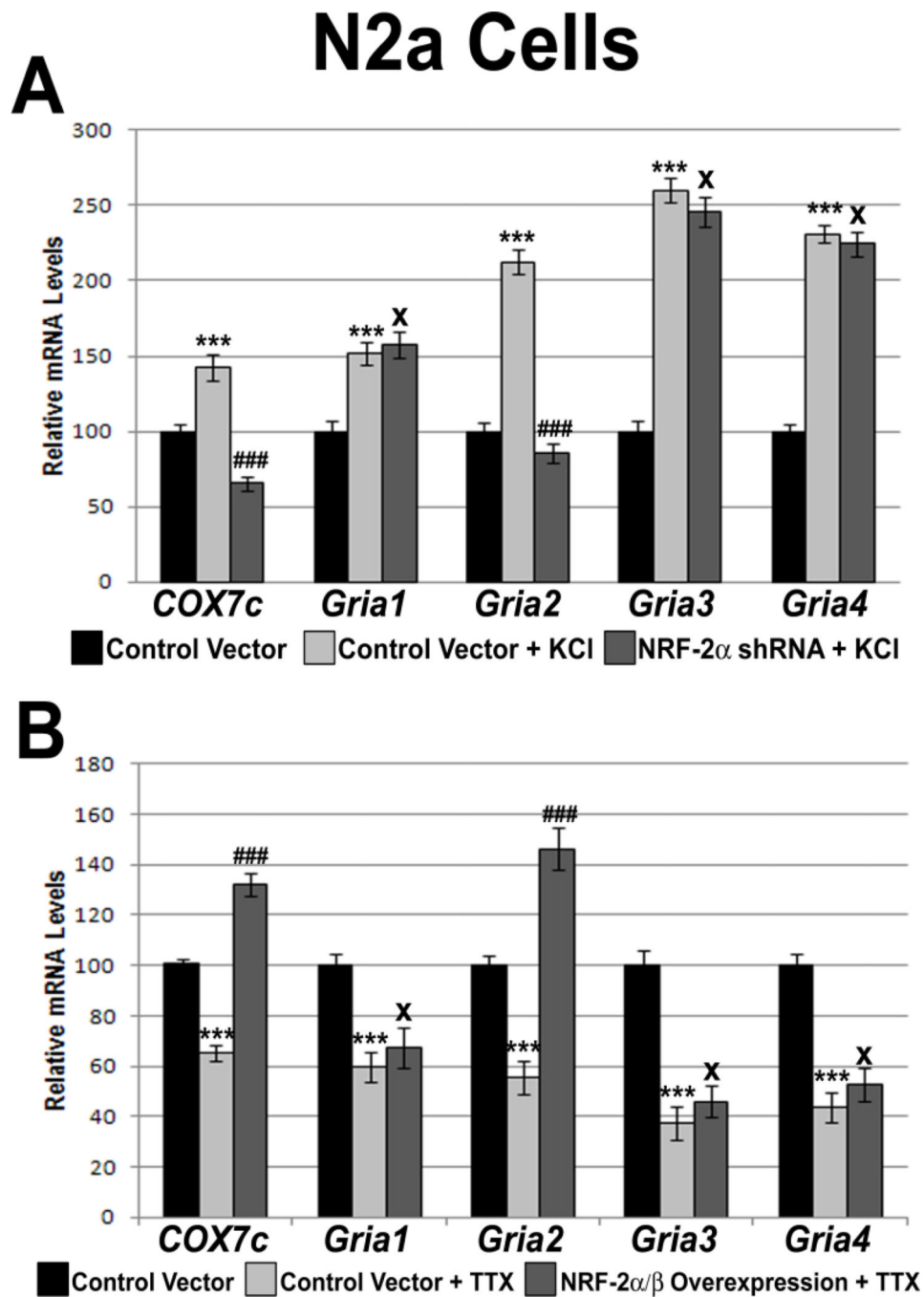


Figure 6. Effect of KCl or TTX treatment in the presence of NRF-2 silencing or over-expression, respectively, on the transcript levels of the AMPA receptor subunit genes and *COX7c* in N2a cells (A) Cells treated for 5 h with 20 mM KCl revealed an up-regulation of all transcripts as compared to pBS/U6 empty vector controls. In the presence of shRNA against NRF-2 α , 5 h treatment with 20 mM KCl failed to up-regulate the transcripts of *Gria2* and *COX7c*, but it did up-regulate those of *Gria1*, *Gria3*, and *Gria4*. (B) N2a cells treated for 3 days with 0.4 μ M TTX revealed a down-regulation of all tested transcripts as compared to pcDNA3.1

empty vector controls. Over-expression of NRF-2 α and β rescued the down-regulation of the *COX7c* and *Gria2* transcripts, but not those of *Gria1*, *Gria3*, and *Gria4*. N = 6 for each data point; *** = $P < 0.001$ when compared to controls; ### = $P < 0.001$ and X = non-significant when compared to KCl- or TTX-treated samples.

Primary Neurons

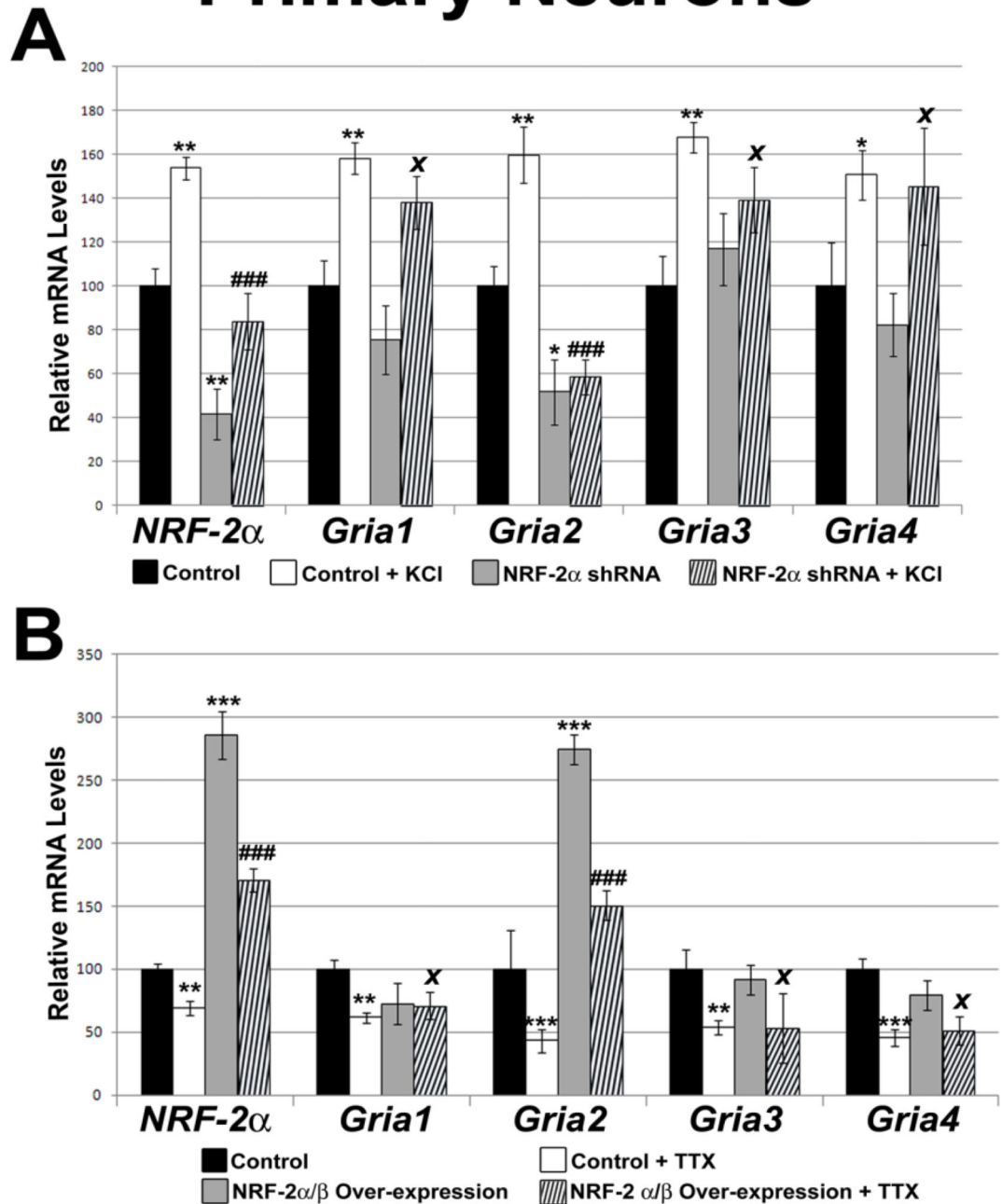


Figure 7.

Effect of NRF-2 silencing and over-expression, with and without KCl or TTX treatment, respectively, on the transcript levels of the AMPA receptor subunit genes in visual cortical neurons. (A) NRF-2 α shRNA transfection in primary neurons down-regulated mRNA levels of *NRF-2 α* and *Gria2*, but not those of *Gria1*, *Gria3*, and *Gria4*. Primary neurons treated for 5 h with 20 mM KCl revealed an up-regulation of all transcripts as compared to pBS/U6 empty vector controls. In the presence of shRNA against NRF-2 α , 5 h treatment with 20 mM KCl did not up-regulate transcripts of *NRF-2 α* and *Gria2*, but it did up-regulate those

of *Gria1*, *Gria3*, and *Gria4*. N = 3 for each data point. ***= $P < 0.001$, **= $P < 0.01$ and *= $P < 0.05$ when compared to pBS/U6 empty vector controls. ### = $P < 0.001$ and X = non-significant when compared to KCl- treated samples. (B) In primary neurons, NRF-2 α / β over-expression led to an increase in the transcript levels of NRF2 α and *Gria2*, but not those of *Gria1*, *Gria3*, and *Gria4*. Primary neurons treated for 3 days with 0.4 μ M TTX revealed a down-regulation of all tested transcripts as compared to pcDNA3.1 empty vector controls. Over-expression of NRF-2 α and β rescued the down-regulation of *Gria2* transcripts, but not those of *Gria1*, *Gria3*, and *Gria4*. N = 3 for each data point; ***= $P < 0.001$ and **= $P < 0.01$ when compared to controls; ### = $P < 0.001$ and X = non-significant when compared to TTX-treated samples.

Gria2

Mouse	-361	CGG <u>CTTCCT</u> AGGCATAGCAACCGGAAATCA	-331
Rat		CGG <u>CTTCCC</u> AGGCATAGCAACCGGAAATCA	
Human		AGG <u>TTTCC</u> -AGGAATGAGCTT- <u>GGAA</u> AAG	

Figure 8.

Aligned partial sequences of *Gria2* promoter from mouse, rat, and human showed conservation of the NRF-2 binding site.

Table 1

A: EMSA Probes. Positions of probes are given relative to TSP. Putative NRF-2 binding sites are underlined.		
Gene Promoter	Position	EMSA Sequence
<i>Gria1</i>	+198/+221	F: 5' TTTTAGAAGGAAGGGAGGAAGGAAAGAA 3'
		R: 5' TTTTTTCTTTCCTTCCCTCCCTTCCCTTCT 3'
<i>Gria2</i>	-327/-298	F: 5' TTTTCGGCTTCCTAGGCATAGCAACCGGAAATCA 3'
		R: 5' TTTTGTGATTTCCGGTTGCTATGCCTAGGAAGCCG 3'
<i>Gria3</i>	+101/+117	F: 5' TTTTGGGTGGAAGGAAAGAGT 3'
		R: 5' TTTTACTCTTCCTTTCCACCC 3'
<i>Gria4</i>	+403/+420	F: 5' TTTTGGGGGAAAGGGAATGGG 3'
		R: 5' TTTTCCCATTCCTTTCCCCCA 3'
<i>COX6b</i>	-47/-23	F: 5' TTTTTCCTCTTGACGCTTCGGCCAGTC 3'
		R: 5' TTTTGACTGGCCGGAAGCTGCAAGAGGA 3'

B: Mutant EMSA Probes. Positions of probes are given relative to TSP. Mutated NRF-2 binding sites are underlined.		
Gene Promoter	Position	Sequence
<i>Gria1</i>	+198/+221	F: 5' TTTTAGAATTTTGGGAGGTTTTAAAGAA 3'
		R: 5' TTTTTTCTTTAAAACCTCCCAAAATCT 3'
<i>Gria2</i>	-327/-298	F: 5' TTTTCGGCAAAATAGGCATAGCAACCTTTTATCA 3'
		R: 5' TTTTGTATAAAAGGTTGCTATGCCTATTTTGCCG 3'

Table 2

Primers and conditions used for ChIP analysis.

Gene Promoter	Position of PCR Product	Sequence
<i>Gria1</i>	+166/+323	F: 5' TCCCCTTCCAAGAGAAACAA 3'
		R: 5' AAAAGAAGCCCTGGTCCAAC 3'
<i>Gria2</i>	-451/-234	F: 5' AGGCAGAAGGCAGTGTGTG 3'
		R: 5' GCTGAGGTTGCAGGGTTTAC 3'
<i>Gria3</i>	-29/+169	F: 5' GGGGTGTGAGAGAGATCCTG 3'
		R: 5' AAGAATTCGCCGGCTCTTAC 3'
<i>Gria4</i>	+264/+513	F: 5' CTCCAGAGCCGGTTCCTC 3'
		R: 5' GGGCTACAGCATCCCTGAG 3'
<i>COX6b</i>	-187/+44	F: 5' AAAGTGCGCAGGCGCTGGAG 3'
		R: 5' CCGAGACGCTGACAGCACCG 3'
Exon 8 of <i>NRF-1</i>		F: 5' GTGGAACAAAATTGGGCCAC 3'
		R: 5' CTGTTAAGGGCCATGGTGA 3'

Table 3

A: Primers used for promoter cloning analysis.		
Gene Promoter	Position	Primer
<i>Gria2</i>	-947/+152	F: 5' CAGACGCGTCCCAAGCAGGCTCGGTGTAATGA 3'
		R: 5' CAGAGATCTGCTGTGGTCCCGGTGTCTGG 3'
<i>COX6b</i>	-291/+44	F: 5' TTGGTACCACTCTGCAGACAGCCTCAC
		R: 5' TTAAGCTTCGGAGCAGCGTTACTTCAAT

B: Primers used for promoter mutagenesis analysis. Mutated NRF-2 binding sites are underlined.		
Gene Promoter	Position	Primer
<i>Mut. NRF-2 Gria2</i>	-333/-288	F: 5' GCAGTTCGGCT <u>IGCT</u> TAGGCATAGCAACCGT <u>ACAT</u> CAGTTTTGCAGC 3'
		R: 5' GCTGCAAAACTGAT <u>GTAC</u> GGTTGCTATGCCTA <u>AGCAG</u> CCGAACTGC 3'
<i>Mut NRF-2 COX6b</i>	-35/-32	F: 5' TCTCCTCTTGCAGCT <u>AGAG</u> GCCAGTCGGAATTCCG 3'
		R: 5' CGGAATTCGGACTGGCT <u>CT</u> AGCTGCAAGAGGAGA 3'

Table 4NRF-2 α and NRF-2 β Cloning Primers

Gene	Primer
<i>NRF-2α</i>	F: 5' AAGCTTACTCCAGCCATGACTAAAAG3'
	R: 5' GGTACCAGCTATACTTGCTCTAAACAT3'
<i>NRF-2β</i>	F: 5' TTGCGGCCGCGATGTCCCTGGTAGATTTG 3'
	R: 5' AAGGATCCTTAAACAGCTTCTTTATTAGTC 3'

Table 5

Real Time Primers

Gene	Primer
<i>Gria1</i>	F: 5' GAGCAACGAAAGCCCTGTGA 3'
	R: 5' CCCTTGGGTGTCGCAATG 3'
<i>Gria2</i>	F: 5' AAAGAATACCCTGGAGCACAC 3'
	R: 5' CCAAACAATCTCCTGCATTTCC 3'
<i>Gria3</i>	F: 5' TTCGGAAGTCCAAGGAAAGT 3'
	R: 5' CACGGCTTTCTCTGCTCAATG 3'
<i>Gria4</i>	F: 5' GGCTCGTGTCCGCAAGTC 3'
	R: 5' TTCGCTGCTCAATGTATTCATTC 3'
<i>COX7c</i>	F: 5' ATGTTGGGCCAGAGTATCCG 3'
	R: 5' ACCCAGATCCAAAGTACACGG 3'
<i>NRF2-α</i>	F: 5' CTCCCGCTACACCGACTAC 3'
	R: 5' TCTGACCATTGTTTCCTGTTCTG 3'
<i>NRF2-β</i>	F: 5' ACCAACCAGTGGGATGGGTCAG 3'
	R: 5' GCACATTCCACCCGGCTCTCAAT 3'
<i>Actb</i>	F: 5' GTGACGTTGACATCCGTAAAGA 3'
	R: 5' GCCGGACTCATCGTACTCC 3'
<i>Gapdh</i>	F: 5' AGGTCGGTGTGAACGGATTTG 3'
	R: 5' GGGTCGTTGATGGCAACA 3'